Analytical Methods

Accepted Manuscript

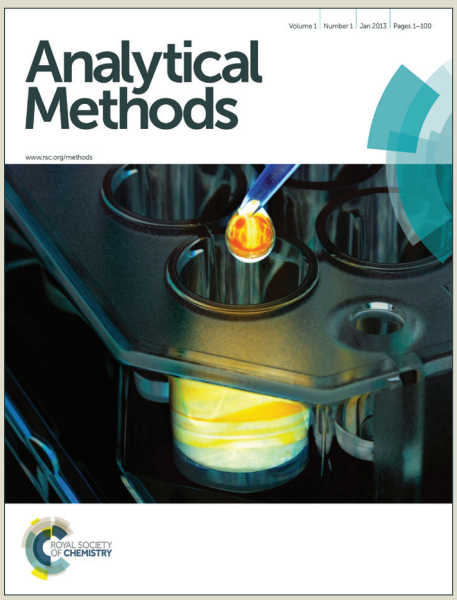

ROYAL SOCIETY OF CHEMISTRY

www.rsc.org/methods

The graphene (GR) and Cysteinc acid (CA) composite (CA/GR) was fabricated through electrochemical method for the modification of glassy carbon electrode (GCE). The obtained detection linearity of isoniazid at CA/GR/GCE was ranging from 0.1 to 200 μM with the detection limit of 0.03 μM (S/N = 3).

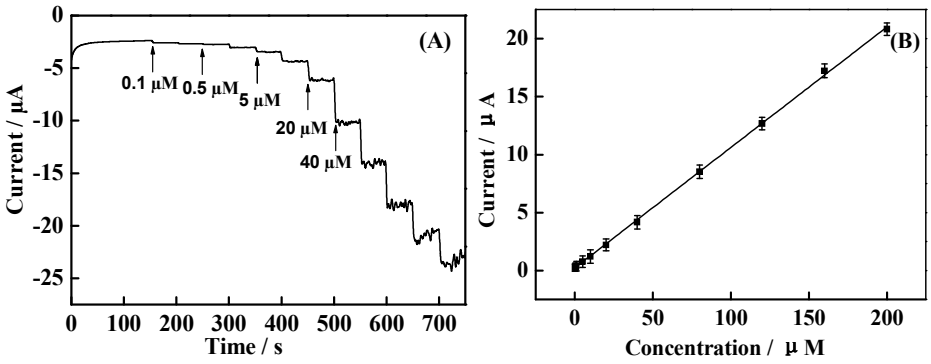

Determination of Isoniazid on Cysteic acid/Graphene Modified Glassy Carbon Electrode

Xiaojing Si [a,b], Lin Jiang [a], Xinyue Wang [a], Yaping Ding [a,*], Liqiang Luo [a]

[a] School of Materials Science and Engineering, School of Sciences, Shanghai University, Shanghai 200444, PR China

[b] School of Public Health, Shanghai Aurora College, Shanghai 201908, PR China

Abstract: The electrodeposited graphene (EGR) and cysteinc acid (CA) composite (CA/EGR) was fabricated through electrochemical method for the modification of glassy carbon electrode (GCE). Fourier transform infrared spectroscopy (FT-IR) was carried out to characterize the proposed CA film. The electrochemical performance of the CA/EGR modified GCE (CA/EGR/GCE) was demonstrated with cyclic voltammetry (CV) and electrochemical impedance spectroscopy (EIS). The modified GCE was designed to act as the electrochemical sensor of isoniazid. The obtained detection linearity at CA/GR/GCE was ranging from 0.1 to 200 μM with the detection limit of 0.03 μM (S/N = 3). Moreover, the sensor was employed for practical sample analysis with satisfied recoveries, further validating the reliable practicability for electroanalysis. Additionally, CA/EGR/GCE also displayed good reproducibility, high stability and excellent anti-interference ability for the determination of isoniazid.

Keywords: Graphene; Cysteinc acid; Isoniazid; Cyclic Voltammetry

* *Corresponding author. Tel.: +86-21-66134734; Fax: +86-21-66132797.*

Address: Department of Chemistry, Shanghai University, Shanghai 200444, PR China.

E-mail address: wdingyp@sina.com (Y. Ding)

1. Introduction

Isoniazid (Scheme 1) is an effective tuberculostatic drug that has been widely used for the treatment of clinical tuberculosis. Also, it is usually used together with other antituberculostatic agents to resist the mycobacterium strains [1−4]. It is undeniable that isoniazid is an essential and indispensable basic remedy for tuberculosis in modern medicine. However, the side effects of isoniazid have long perplexed both the patients and curer. Specifically, toxicity such as hepatotoxicity and nervous system toxicity, therapeutic failure, relapse and multiple drug resistance are associated with isoniazid ingestion [5−6]. Worse still, hydrazine produced during the isoniazid metabolism not only induces hepatotoxicity with inflammation but also can lead to death [7]. Therefore, it is of vital importance to develop sensitive, rapid and reliable analytical methods to determine isoniazid in clinical and pharmaceutical treatment.

<Scheme 1 here>

Till now, many methods have been reported for the determination of isoniazid, including spectrophotometry [8,9], electrochemiluminescence [10,11], high performance liquid chromatography [12,13], capillary electrophoresis [14] and electrochemical technique [15−18]. Among these methods mentioned, the electrochemical technique has received increasing attention because of its fast response, easy handling, excellent conductivity and low costs. However, the electrochemical detection of isoniazid on bare electrode was not optimal since the bare surface of electrode is sluggish to transfer electrons and vulnerable to contaminate [19]. To overcome these problems, various chemically modified electrodes have been designed, such as the poly(amidosulfonic acid) modified glassy carbon electrode [2], overoxidized polypyrrole modified glassy carbon electrode [3], poly(3,4-ethylenedioxy thiophene) electrode [15] and ordered mesoporous carbon modified electrode [16]. Among these modified electrodes, conducting polymer modified electrode has attracted attention in recent years due to its good stability, excellent permselectivity, more active sites and strong adherence to electrode surface that could promote the electron-transfer processes and minimize this contamination [20].

Graphene (GR), a flate monoplayer of sp^2-bonded carbon atoms packed into a honeycomb two-dimensional lattice, has attracted fascinating interests across different disciplines due to its remarkable and extraordinary structural, physical and chemical properties [21−26]. Especially, the unique electronic properties makes GR be an excellent alternative material in designing electrochemical sensors. The GR-oriented electrochemical modified electrodes have received increasing attention due to the combination of the ultrahigh specific surface area, ambipolarity, better reproducibility and unique electronic features in recently years [27−31]. Among them, potentiostatic methods can minimize the thickness of GR film and reduce the probability of side reactions. During the electrodepositing process, few layers of GR with crimple effect were deposited and oxidized on the surface of electrode which could be highly beneficial in maintaining a high effective surface area on the electrode [32].

L-Cysteine (L-Cys) is an important amino acid owing to its crucial roles in biological systems. Due to the presence of sulfhydryl, L-Cys could be electrochemically oxidized to cysteic acid (CA) and form a thin, conductive film at the surface of electrode [33]. According to previous reports, various types of electrode modified with CA have been utilized to determine drugs with good detection results, such as terbinafine, sinomenine, nimesulide, meloxicam, adenine and theophylline [34−40].

In this work, a facile and novel preparation strategy based on electrochemical techniques for the fabrication of CA/EGR modified glassy carbon electrode (CA/EGR/GCE) was developed. CA was prepared by electrochemical oxidation of L-Cys on the surface of the electrode. It was found that the oxidation peak current of isoniazid on CA/EGR/GCE is much higher over that on bare GCE. The proposed electrode was successfully employed to detect the concentration of isoniazid in pharmaceutical formulations and human serum samples.

2. Experimental

2.1 Chemicals

GR was purchased from XFNANO Materials Tech Co., Ltd (Nanjing, China). Isoniazid was obtained from Aladdin Chemical Reagent Co., Ltd. (Shanghai, China) and the isoniazid tablets were supported by Yunpeng pharmaceutical Co., Ltd. (Shanxi, China). All chemicals employed in this work were of analytical grade and obtained from Sinopharm Group Chemical Reagent Co., Ltd. (Shanghai, China). All experiments were performed in 0.1 M phosphate buffer solution (PBS) and double distilled water was used throughout the experiment. All experiments were carried out at room temperature.

2.2 Apparatus

All the electrochemical measurements including cyclic voltammetry (CV), electrochemical impedance spectroscopy (EIS), chronoamperometry were carried out on a CHI 660D electrochemical workstation (Chenhua Corp. Shanghai, China). A conventional three-electrode system was used for all electrochemical experiments, which consisted of a GCE (Φ = 3 mm) coated with CA/EGR/GCE film as the working electrode, a platinum electrode as the counter electrode and a saturated calomel electrode as the reference electrode. Fourier transform infrared spectra (FT-IR) were carried out on AVATAR 370 Fourier transform infrared spectrometer (USA).

2.3 Preparation of modified electrodes

A bare GCE was polished to a mirror-like surface with alumina slurries prior to electrochemical modification. After being rinsed with water, the GCE was ultrasonicated in HNO_3 solution (v/v, 1:1), ethanol and double distilled water for 5 min, sequentially.

200 μL GR (1 mg mL^{-1}) was added into 10 mL KCl (0.1 M) with ultrasonication for 15 min to form a homogeneous suspension. The EGR/GCE was gained *via* eletro-deposition at a potentiostatic potential of +1.7 V for 400 s in GR solution. Then the resultant electrode was immersed into 0.1 M PBS (pH 7.0) with 0.5 mM L-Cys for further immobilization by CV in the potential range of –0.8 – 2.2 V at 100 mV s^{-1} for 10 cycles. Finally, the EGR/CA/GCE was obtained and washed with double distilled water carefully for further use.

2.4. Treatment of samples

2.4.1. Tablets

Several tablets of isoniazid were powdered in a mortar. An accurately weighed portion of the powder was dissolved and transferred into a 100 mL volumetric flask with 0.01M HCl. Then the obtained solution was further diluted to be 1 mg mL^{-1} for sample determination. The sample solution was stored at 4 ℃.

2.4.2. Human serum samples

Fresh serum samples from healthy person were provided by Shanghai University Hospital. A mixture of 1 mL blood sample and 0.15 mL perchloric acid was centrifuged at 2500 rpm for 15 min with the aim of removing redundant protein. After that, the supernatant was directly injected to PBS (pH 3.5) to give a total volume of 10 mL for the drug determination in human serum.

All experiments were performed in compliance with the relevant laws and institutional guideline, under the approval of the institutional ethics committee.

3. Results and discussion

3.1 IR and EIS characterization

The oxidation reaction mechanism of L-Cys to CA on electrode has been reported [41−44]. In this work, L-Cys powder sample and CA film sample were characterized by FT-IR in order to verify the formation of CA on the GCE. As shown in the spectra of L-Cys (curve a) in Fig. 1, the absorption bands in the range of 2500 to 3500 cm^{-1} were attributed to the ν (C-H) and ν (N-H) stretching vibration absorptions. Besides, the R-COO− asymmetric and symmetric stretching vibration absorptions were respectively observed at 1586 and 1394 cm^{-1}. A band at 2550 cm^{-1} corresponded to S-H stretching vibration [45]. While in the spectra of CA (curve b), the fine structures of L-Cys in curve a disappeared. Specifically, the S-H stretching vibration at 2550 cm^{-1} vanished, which implied S-H was oxidized to SO_3H. The peaks at 2984 cm^{-1} (C-H, N-H stretching vibration) obviously broadened due to electrochemical reaction of L-Cys. Additionally, the peak at 1639 cm^{-1} was a combination of the peaks of C=O and C=C stretching vibrations and the peak at 1116 cm^{-1} corresponded to the association of three C-N stretching vibration in curve b. To sum up, all of these results indicate that L-Cys has been successfully oxidized to CA on the GCE.

<Fig.1 here>

In order to probe the electrochemical properties of EGR and CA, EIS was performed in 5.0 mM $K_3Fe(CN)_6/K_4Fe(CN)_6$ (1:1) containing 0.1 M KCl using an alternating current voltage of 0.01 V and being recorded at a bias potential of 0.2 V within a frequency range from 10^{-1} to 105 Hz. In general, the Nyquist plot of EIS consists of a semicircle portion at higher frequencies and a linear portion at lower frequencies, which correspond to the electron transfer limited progress and the diffusion progress, respectively. The typical Nyquist plots of bare GCE, EGR/GCE and CA/EGR/GCE were shown in Fig.2. The apparent charge transfer resistance (Rct) value was measured as the diameter of the semicircle in the Nyquist plots. An increase in Rct value indicates a resistance or hindrance of electron flow due to the addition of a substance on the surface of the electrode. The Rct of EGR/GCE was smaller than that of bare GCE, indicating that EGR is vital to accelerate the transfer of the electrons on the surface of GCE. After incorporating EGR with CA, the Rct of the obtained electrode increased markedly, reflecting that it's hard to transfer electron at the CA/EGR/GCE. All the phenomena revealed that EGR and CA were well attached to the electrode surface and changed the electrochemical properties of the electrode/electrolyte surface of electrode.

<Fig.2 here>

3.2 Electrochemical response of CA/EGR/GCE for isoniazid

Fig. 3 shows cyclic voltammograms of the bare GCE (a), EGR/GCE (b), CA/GCE(c) and CA/EGR/GCE (d) in 0.1 M PBS (pH 3.5) containing 10 μM isoniazid at the scan rate of 100 mV s^{-1}. It was observed that there is no oxidation current on bare GCE, which may be attributed to the poor electrochemical activity of isoniazid at bare electrode. However, the peak current both increased dramatically with the introduction of EGR and CA. Moreover, the peak current of isoniazid reached the greatest value at CA/EGR/GCE with 8-fold's improvement than that at bare GCE. All the results indicate that the electrocatalytic activity of GCE towards isoniazid was highly boosted by the CA and EGR composite.

<Fig.3 here>

The effect of scan rate (0.020 − 0.220 V s^{-1}) on the electrocatalytic oxidation of 20 μM isoniazid at the CA/EGR/GCE was investigated by CV (Fig. 4). As can be observed in Fig. 4A, the oxidation peak potential of isoniazid shifted positively

with the increase of the scan rate confirming the kinetic limitation in the electrochemical reaction. Also, as shown in Fig. 4B, the oxidation peak current is linear to the square root of the scan rate, which could be described by the following equation: $Ip/\mu A = 47.6260\ (\upsilon/V\ s^{-1})^{1/2} - 3.8216$ (R = 0.9957). This result suggests that the process of isoniazid oxidation is controlled by diffusion.

<Fig.4 here>

3.3 Optimization of CA/EGR/GCE performance for isoniazid

3.3.1 Effect of solution pH

The pH of solution has an important effect on the electrochemical behaviors of isoniazid, including the oxidation peak currents and the oxidation peak potentials. The influence of pH on the electrochemical behavior of isoniazid at CA/EGR/GCE has been investigated in 0.1 M PBS containing 20 μM isoniazid by CV (Fig. 5). As shown in Fig. 5B, the oxidation current of isoniazid peaked at pH 3.5, and then steeply decreased after that. Hence, pH 3.5 has been chosen as the optimal condition for the buffer solution.

<Fig.5 here>

3.3.2 Effect of Electro-polymerization cycles of L-Cys

The modification time is another key factor impacting on the electrochemical performance of the proposed sensor. Fig. 6 exhibits the effect of electro-polymerization cycle of L-Cys on the current response of 20 μM isoniazid in 0.1 M PBS (pH 3.5). As shown in Fig.6, when the electro-polymerization cycle increased from 5 to 10, the oxidation current of isoniazid increased as more CA film was generated at EGR/GCE. Then the oxidation current of isoniazid decreased gradually as the cycles were more than 10. Therefore, 10 electro-polymerization cycles of L-Cys is selected as the optimum modification time to construct the proposed sensor of isoniazid.

<Fig.6 here>

3.4 Calibration curve

Under the optimal conditions, I-t technique was selected to research the linear relevance between the concentration of isoniazid and its oxidation current (Fig. 7). The response current was obtained at an optimized applied potential of 0.39 V via successive additions of isoniazid into a stirring PBS solution (pH 3.5). The oxidation peak currents of isoniazid increased linearly with concentration in the range of 0.1 − 200 μM. The relationship can be described as follows: $Ip\ /\mu A = 0.1976 + 0.1042C\ /\mu M$ with a correlation coefficient of 0.9998. The detection limit (S/N = 3) and the sensitivity is calculated to be 0.03 μM and 1474.88 $\mu A \cdot mM^{-1} \cdot cm^{-2}$, respectively.

<Fig.7 here>

The comparison of proposed method with other methods [2,15,46−49] used in the determination of isoniazid is listed in Table 1, which demonstrated our method owned lower detection limit and competitive linear range for determination compared with most reported papers.

< Table 1 here>

3.5 Interference, reproducibility and stability

Under optimized conditions, the effects of different interfering substances on the determination of 1 μM isoniazid at CA/EGR/GCE were evaluated in detail to investigate the anti-interference ability of the proposed sensor. The tolerance limit is defined as the maximum concentration of the interference substances that can bring ±5 % relative error in the detection. Table 2 shows that NaCl, $CaCl_2$, KNO_3, glucose, sucrose, leucine, lysine, phenylalanine, glutamic acid, glycine, uric acid, dopamine, ascorbic acid had almost no influence on the current responses of isoniazid. All these indicated that the proposed sensor has good selectivity to the determination of isoniazid.

< Table 2 here>

The reproducibility was explored by five repetitive and successive measurements of isoniazid at a same CA/EGR/GCE by CV. The relative standard deviation (RSD) (n = 5) was calculated to be 4.67%.

The stability of CA/EGR/GCE was investigated by storing the modified electrode in a refrigerator at 4 □ for seven days. Finally, 4.94% loss of the oxidation peak current of isoniazid was obtained. These data demonstrate that the proposed sensor has an excellent stability and reproducibility for the isoniazid determination.

3.6 Real samples analysis

In order to verify the applicability of the proposed sensor, CA/EGR/GCE was utilized to detect the isoniazid content in pharmaceutical formulations and human serum samples by I-t technique, respectively. The results are summarized and listed

in Table 3. Satisfactory recoveries for real samples demonstrated that the proposed sensor held great promise for reliable and sensitive application in the field of pharmaceutical and clinical analysis.

<Table 3 here>

4. Conclusion

In summary, we have proposed a novel and simple preparation strategy for the modification of GCE with EGR and CA and demonstrated its applicable feasibility as an electrochemical sensor of isoniazid for the fist time. The enhanced electrocatalytic activity of isoniazid at CA/EGR/GCE is mainly attributed to the excellent conductivity and large surface area of EGR combined with the functional polymer of CA. Moreover, the proposed sensor has displayed good sensitivity, reproducibility and stability. With the proved electroanalytic performance, we have successfully utilized CA/EGR/GCE to determine isoniazid in pharmaceutical formulations and human serum samples with satisfied results.

Acknowledgements

This research is supported by the National Natural Science Foundation of China (Nos. 21271127, 61171033), the Nano-Foundation of Science and Techniques Commission of Shanghai Municipality (Nos. 12nm0504200, 12dz1909403).

References

[1] G.K. Mcevory (Ed.), *American Society of Hospital Pharmacists,* 1990, 344–348.
[2] G.Yang, C. Wang, R. Zhang, C. Wang, Q. Qu, X. Hu, *Bioelectrochem.* 2008, **73**, 37−42.
[3] M.R. Majidi, A. Jouyban, K. Asadpour-Zeynali, *J. Electroanal. Chem.* 2006, **589**, 32–37.
[4] S. Yao, W. Li, X. Su, X. Zuo, W. Wei, *Talanta.* 1999, **50**, 469–480.
[5] C.M. Nolan, S.V. Goldberg , S.E. Buskin, *J. Am. Med. Assoc.* 1999, **281**, 1014–1018.
[6] J.Ray, I. Gardiner, and D. Marriott, *Intern. Med. J.* 2003, **33**, 229–234.
[7] S. Tafazoli, M. Mashregi and P. J. O'Brien, *Appl. Pharmcol*, 2008, **229**, 94–101.
[8] H.C. Goicoechea, A.C. Olivieri, *J. Pharm. Biomed. Anal.* 1999, **20**, 681 – 686.
[9] P. Nagaraja, K.C.S. Murthy, H.S. Yathirajan*, Talanta.* 1996, **43**, 1075–1080.
[10] B. Wu, Z. Wang, Z. Xue, X. Zhou, J. Du, X. Liu and X. Lu, *Analyst.* 2012, **137**, 3644–3652.
[11] A. Safavi, M.A. Karimi, M.R.H. Nezhad, *J. Pharm. Biomed. Anal.* 2003, **30**, 1499–1506.
[12] M.Y. Khuhawar, F.M.A. Rind, *J. Chromatogr. B*, 2002, **766**, 357–363.
[13] E. Calleri, E.D. Lorenzi, S. Furlanetto, *J. Pharma. Biomed. Anal.* 2002, **29**, 1089–1096.
[15] T.Y. You, L. Niu, J.Y. Gui, S.J. Dong, E.K. Wang, *J. Pharm. Biomed.Anal.* 1999, **19**, 231–237.
[15] N. F. Atta, A. Galal, R. A. Ahmed, Int. *J. Electrochem. Sci.* 2011, **6**, 5097–5113.
[16] X. Yan, X.J. Bo, L.P. Guo. *Sensor. Actuat. B.* 2011, **155**, 837–842.
[17] W.C. Chen, B. Unnikrishnan, S.M. Chen. *J. Electrochem. Sci.* 2012, **7**, 9138–9149.
[18] Srikanth Cheemalapati, Selvakumar Palanisamy, Shen-Ming Chen. *J. Electrochem. Sci.* 2013, **8**, 3953–3962.
[19] B.O. Agboola, K.I. Ozoemenab and T. Nyokong, *Electrochim. Acta.* 2006, **51**, 6470.
[20] I. Jurevičiūtė, K. Brazdžiuvienė, L. Bernotaitė, et al. *Sensor. Actuat. B-Chem.* 2005, **107**,716-721.
[21] A.K. Geim, K.S. Novoselov, *Nat. Mater.* 2007, **6**, 183–191.
[22] M.D. Stoller, S.J. Park, Y.W. Zhu, J.H. An, R.S. Ruoff, *Nano Lett.* 2008, **8**, 3498–3502.
[23] D.W. Wang, F. Li, J.P. Zhao, W. Ren, Z.G. Chen, J. Tan, Z.H. Wu, I.Gentle, G.Q. Lu, H.M. Cheng, *Nano. Commun.* 2009, **3**, 1745–1752.
[24] S. Stankovich, D. Dikin, R. Piner, K. Kohlhaas, A. Kleinhammes, Y. Jia, Y. Wu, S.Nguyen, R. Ruoff, *Carbon.* 2007, **45**, 1558–1565.
[25] Y. Wang, J. Lu, L. Tang, H. Chang, J. Li, *Anal. Chem.* 2009, **81**, 9710–9715.
[26] Y. Ohno, K. Maehashi, Y. Yamashiro, K. Matsumoto, *Nano Lett.* 2009, **9**, 3318–3322.
[27] A. Gutés, C. Carraro, R. Maboudian, *Biosens. Bioelectron.* 2012, **33**, 56–59.
[28] M. Pumera, A. Ambrosi, A. Bonanni, E.L.K. Chng, H.L. Poh, *Trends Anal. Chem.* 2010, **29**, 954–965.
[29] Y. Guo, Y. Han, S. Shuang, C. Dong, *J. Mater, Chem.* 2012, **22**, 13166–13173.
[30] C. Zhu, Y. Fang, D. Wen, S. Dong, *J. Mater, Chem.* 2011, **21**, 16911–16917.
[31] K. Liu, J.J. Zhang, C. Wang, J.J. Zhu, *Biosens. Bioelectron.* 2011, **26**, 3627–3632.
[32] L. Jiang, S. Gu, Y. Ding, et al. *Nanoscale*. 2014, **6**, 207-214.
[33] F.F Zhang, S.Q Gu, Y.P Ding, L. Li, X. Liu, *Bioelectrochem.* 2013, **89**, 42–49
[34] C.Y. Wang, Y.D. Mao, D.Y. Wang, *Bioelectrochemistry.* 2008, **72**, 107–115.
[35] J. Guan, Z.X.Wang, C.Y.Wang, *Int. J. Electrochem. Sc.* 2007, **2**, 572–582.
[36] C.Y. Wang, Q.X. Liu, X.Q. Shao, *Anal. Lett.* 2007, **40**, 689–704.
[37] C.Y. Wang, X.Q. Shao, Q.X. Liu, *J. Pharm. Biomed. Anal.* 2006, **42**, 237–244.
[38] C.Y. Wang, Z.X. Wang, J. Guan, *Sensors.* 2006, **6**, 1139–1152.
[39] Q. Xu, M. Sun, Q.X. Du, Curr. *Pharm. Anal.* 2009, **5**, 190–196.
[40] B. Brunetti, E. Desimoni, *Electroanalysis.* 2009, **21**, 772–778.
[41] A. Salimi, R. Hallaj, *Talanta.* 2005, **66**, 967–975.
[42] J. Zagal, C. Fierro, R. Rozas, *J. Electroanal. Chem.* 1981, **119**, 403–408.

[43] T.R. Ralph, M.L. Hitchman, J.P. Millington, F.C.Walsh, *J. Electroanal. Chem.* 1994, **375**, 1–15.
[44] S.D. Fei, J.H. Cheng, S.Z. Yao, G.H. Deng, D.L. He, Y.F. Kuang, *Anal. Biochem.* 2005, **339**, 29–35.
[45] I. Feliciano-Ramos, M. Caban-Acevedo, M. Aulice Scibioh, C.R. Cabrera, *J. Electroanal. Chem.* 2010, **650**, 98–104.
[46] M. A. Karimi, A. Hatefi-Mehrjardi, M. Mazloum-Ardakani, et al. *Int. J. Electrochem. Sci.* 2010, **5**, 1634-1648.
[47] S. Shahrokhian, E. Asadian. *Electrochim. Acta*, 2010, **55**, 666-672.
[48] M. F. Bergamini, D. P. Santos, M. V. B. Zanoni. *Bioelectrochemistry*, 2010, **77**, 133-138.
[49] S. Shahrokhian, M. Amiri. *Microchim. Act*a, 2007, **157**,149-158.

Figure Captions:

Scheme 1. Chemical structure of isoniazid.

Fig. 1 FTIR spectra of L-Cysteine powder (a) and CA films (b).

Fig. 2 Nyquist plot of EIS for bare GCE, EGR/GCE and CA/EGR/GCE in 5 mM $K_3[Fe(CN)_6]/K_4[Fe(CN)_6]$ solution.

Fig. 3 Cyclic voltammograms of 0.1 M PBS (pH 3.5) with 10 μM isoniazid at bare GCE (a), EGR/GCE (b), CA/GCE (c) and CA/EGR/GCE (d), insert: Cyclic voltammograms of 0.1 M PBS (pH 3.5) at bare GCE (a), EGR/GCE (b), CA/GCE (c) and CA/EGR/GCE (d).

Fig. 4 (A) Cyclic voltammograms of the CA/EGR/GCE in 0.1 M PBS (pH 3.5) including 20 μM isoniazid at different scan rates (0.020-0.220 V s^{-1}); (B) The linear dependence of peak current with the square root of scan rate.

Fig. 5 (A) Cyclic voltammograms of 20 μM isoniazid in 0.1M PBS with various pH (from 4.5 to 2.5) at CA/ EGR/GCE. (B) The effect of pH value on the oxidation current response of 20 μM isoniazid at CA/ EGR/GCE.

Fig. 6 Effect of electro-polymerization cycles of L-cysteine on the oxidation current response of 20 μM isoniazid.

Fig. 7 (A) Fig. 8 (A) Current-time curve of CA/EGR/GCE at different concentrations of isoniazid (0.1→200 μM); (B) The calibration curve for the determination of isoniazid.

Tables

Table 1 Comparison of major characteristics at different electrodes for determination of isoniazid.

Electrodes	Dynamic range/μM	LOD/μM	References
PASA/GCE	0.05 – 10	0.01	[2]
PEDOT/Pt	10 – 100	0.045	[15]
ARS/GCE	10 – 800	3.94	[45]
CNT/TCPE	1 – 100	0.5	[46]
PH/SPCE	0.5 – 110	0.17	[47]
MWCPE	1 – 1000	0.5	[49]
CA/EGR/GCE	0.1 – 200	0.03	This work

PASA/GCE: poly(amidosulfonic acid) modified glassy carbon electrode; PEDOT/Pt: poly(3,4-ethylenedioxythiophene) modified platinum electrode; ARS/GCE: alizarin red S modified glassy carbon electrode; CNT/TCPE: multi-walled carbon nanotube/thionine modified electrode; PH/SPCE: poly-L-histidine modified screen-printed carbon electrode; MWCPE: multi-walled carbon nanotube paste electrode.

Table 2 The influences of some inorganic salts and important biological substances on the peak current of 1 μM isoniazid at CA/EGR/GCE.

Interferents	Concentration (μM)	Signal change (%)
NaCl	1000	1.90
$CaCl_2$	1000	0.92
KNO_3	1000	1.96
Glucose	500	0.20
Sucrose	500	0.21
Leucine	500	2.88
Lysine	500	1.90
Phenylalanine	500	2.46
Glutamic acid	500	1.85
Glycine	500	2.88
Uric acid	25	1.19
Dopamine	25	1.11
Ascorbic acid	25	4.67

Table 3 Determination of isoniazid in pharmaceutical formulations and human serum samples (n=3).

Samples	Detected （μM）	Added （μM）	Found （μM）	Recovery (%)	RSD (%)
Tablet 1	1.88	10.00	11.50	96.20	0.58
Tablet 2	7.19	10.00	17.61	104.20	2.89
Human serum	-	10.00	9.77	97.70	2.61
	-	20.00	20.08	100.40	2.52

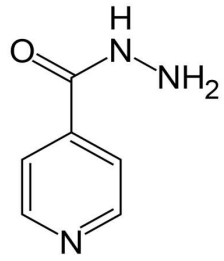

Scheme 1. Chemical structure of isoniazid.

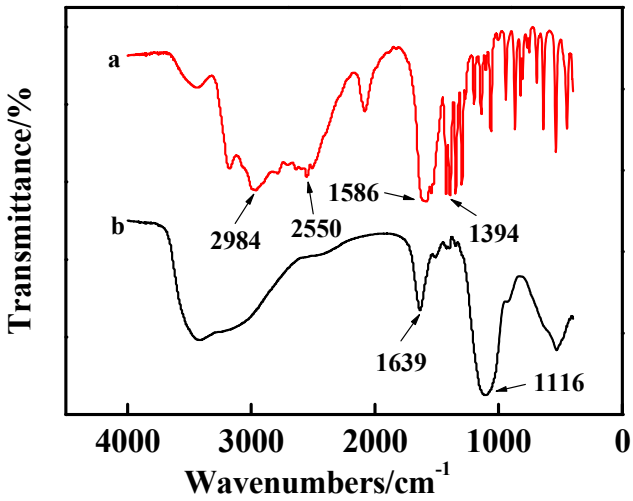

Fig.1 FTIR spectra of L-Cysteine powder (a) and CA films (b).

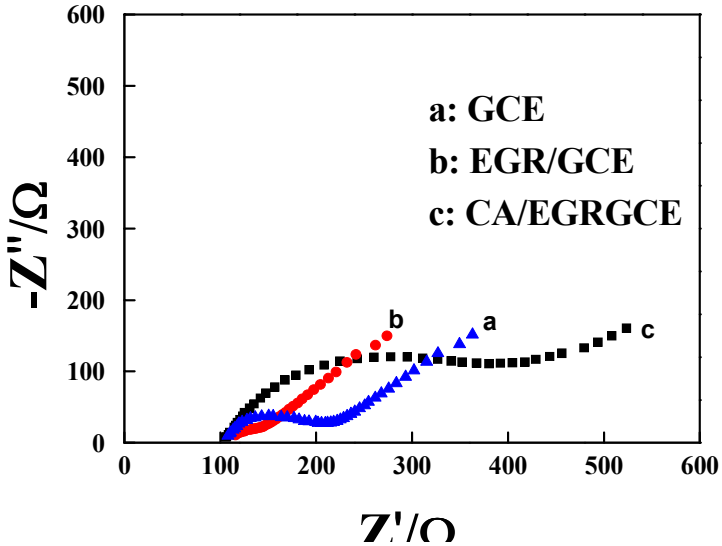

Fig.2 Nyquist plots of EIS for bare GCE, EGR/GCE and CA/EGR/GCE in 5 mM $K_3[Fe(CN)_6]/K_4[Fe(CN)_6]$ solution.

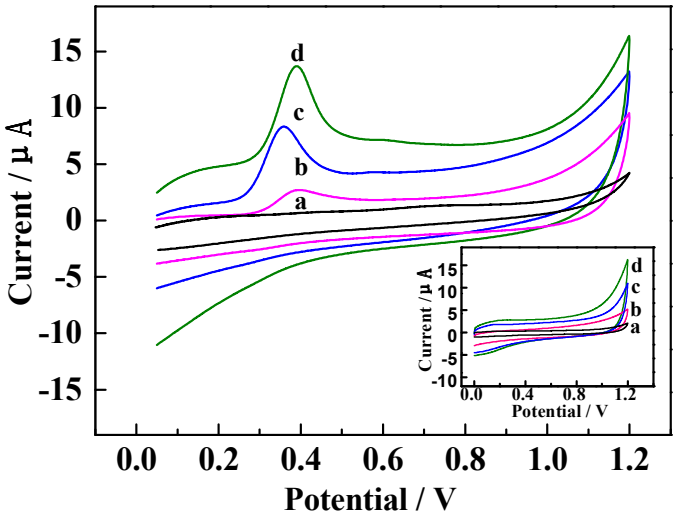

Fig. 3 Cyclic voltammograms of 0.1 M PBS (pH 3.5) with 10 μM isoniazid at bare GCE (a), EGR/GCE (b), CA/GCE (c) and CA/ EGR/GCE (d), insert: Cyclic voltammograms of 0.1 M PBS (pH 3.5) at bare GCE (a), EGR/GCE (b), CA/GCE (c) and CA/EGR/GCE (d).

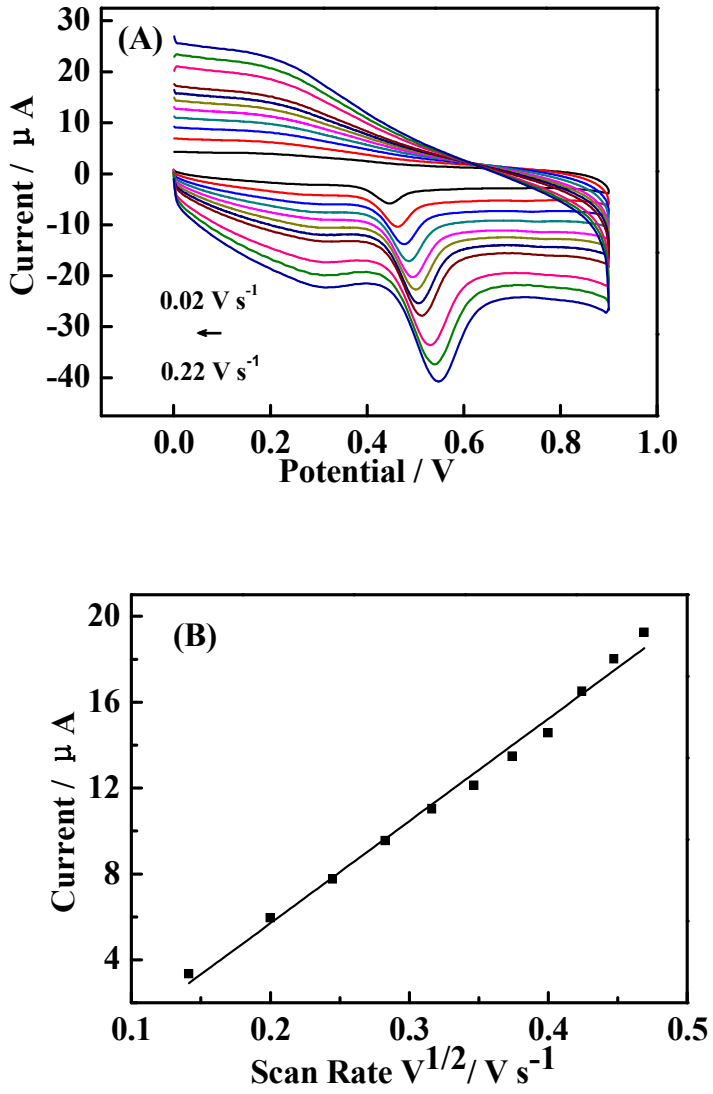

Fig.4 (A) Cyclic voltammograms of the CA/EGR/GCE in 0.1 M PBS (pH 3.5) including 20 μM isonizid at different scan rates (0.020-0.220 V s−1); (B) The linear dependence of peak current with the square root of scan rate.

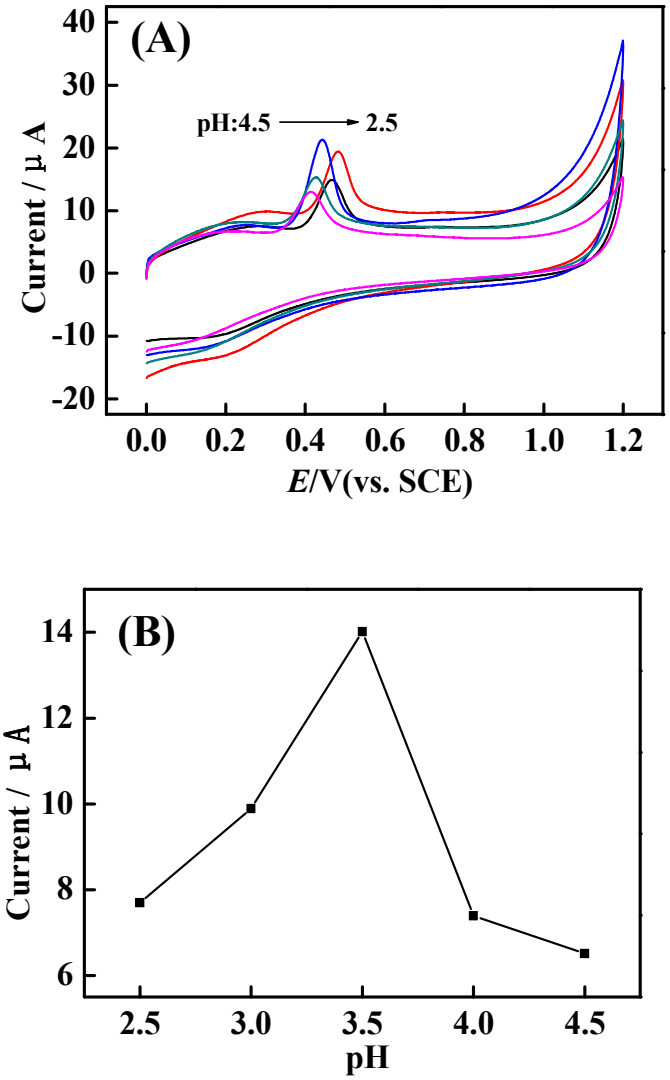

Fig. 5 (A) Cyclic voltammograms of 20 μM isoniazid in 0.1M PBS with various pH (from 4.5 to 2.5) at CA/EGR/GCE. (B) The effect of pH value on the oxidation current response of 20 μM isoniazid at CA/EGR/GCE.

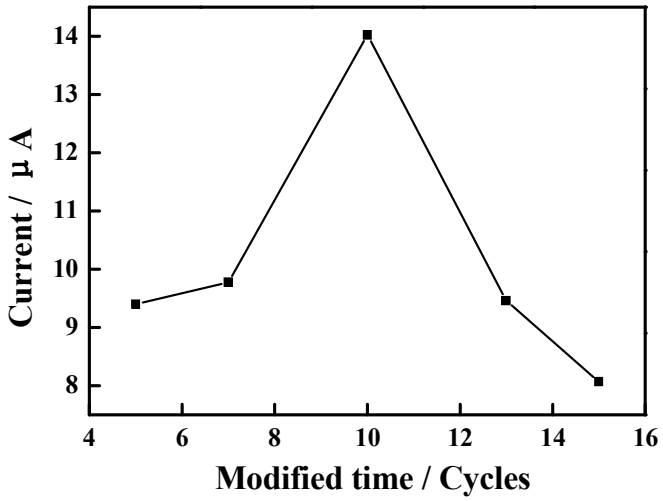

Fig. 6 Effect of electro-polymerization cycles of L-cysteine on the oxidation current response of 20 μM isoniazid.

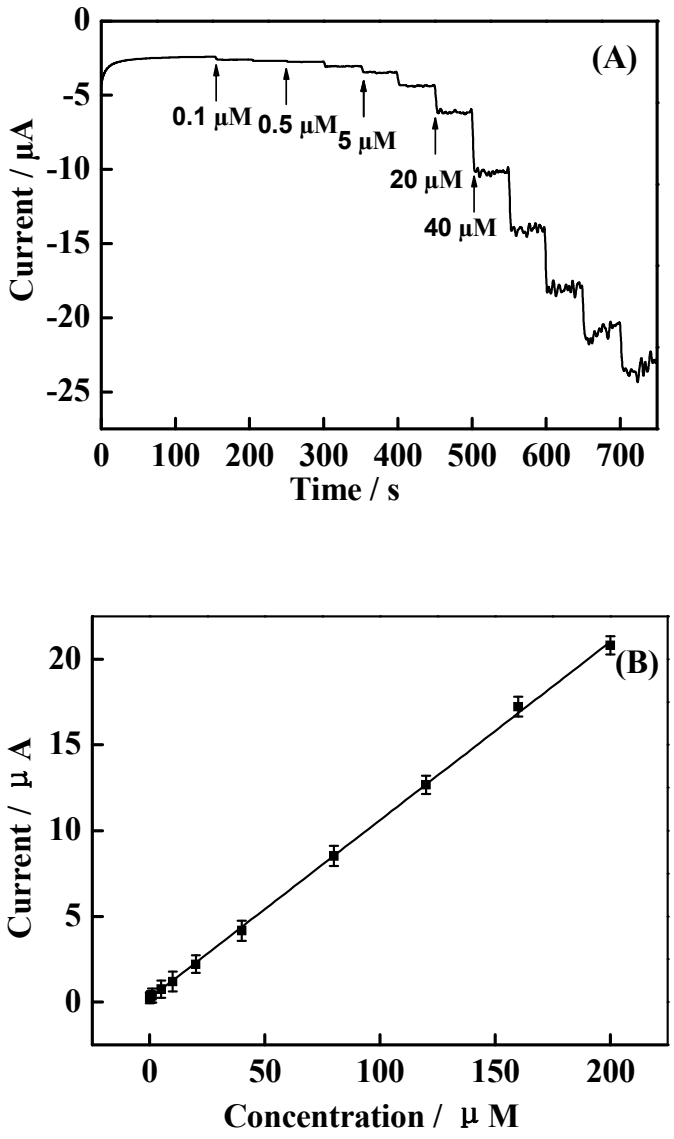

Fig. 7 (A) Current-time curve of CA /EGR/GCE at different concentrations of isoniazid (0.1→200 μM); (B) The calibration curve for the determination of isoniazid.

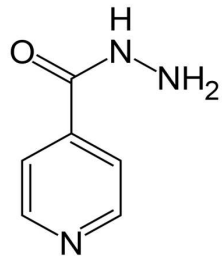

Scheme 1. Chemical structure of isoniazid.

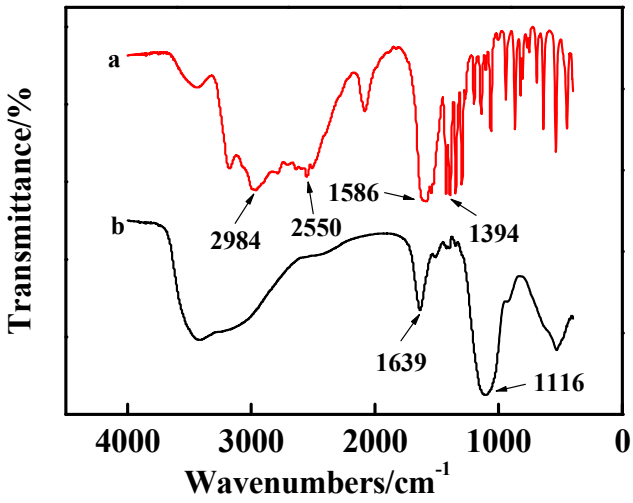

Fig.1 FTIR spectra of L-Cysteine powder (a) and CA films (b).

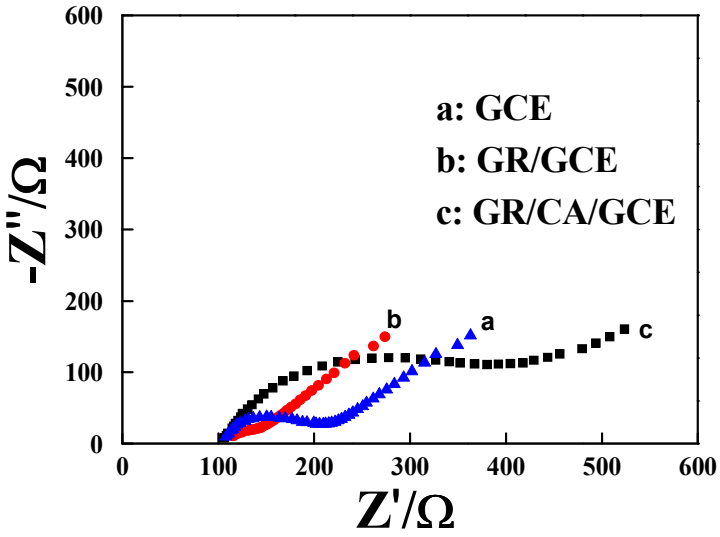

Fig.2 Nyquist plots of EIS for bare GCE, GR/GCE and GR/CA/GCE in 5 mM $K_3[Fe(CN)_6]/K_4[Fe(CN)_6]$ solution.

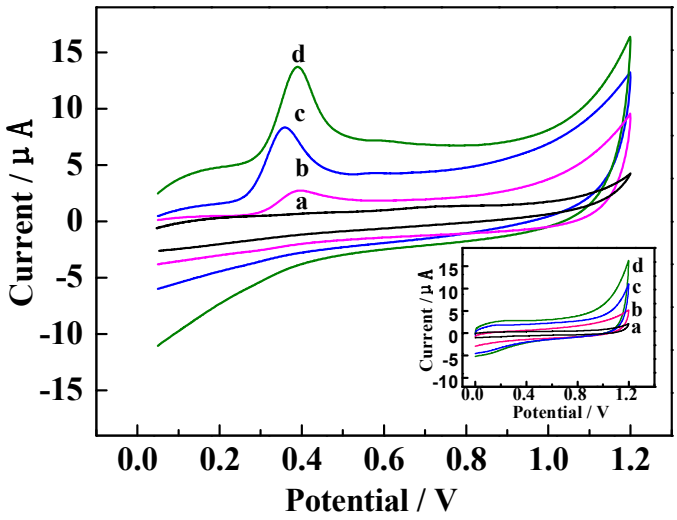

Fig. 3 Cyclic voltammograms of 0.1 M PBS (pH 3.5) with 10 μM isoniazid at bare GCE (a), GR/GCE (b), CA/GCE (c) and GR/CA/GCE (d), insert: Cyclic voltammograms of 0.1 M PBS (pH 3.5) at bare GCE (a), GR/GCE (b), CA/GCE (c) and GR/CA/GCE (d).

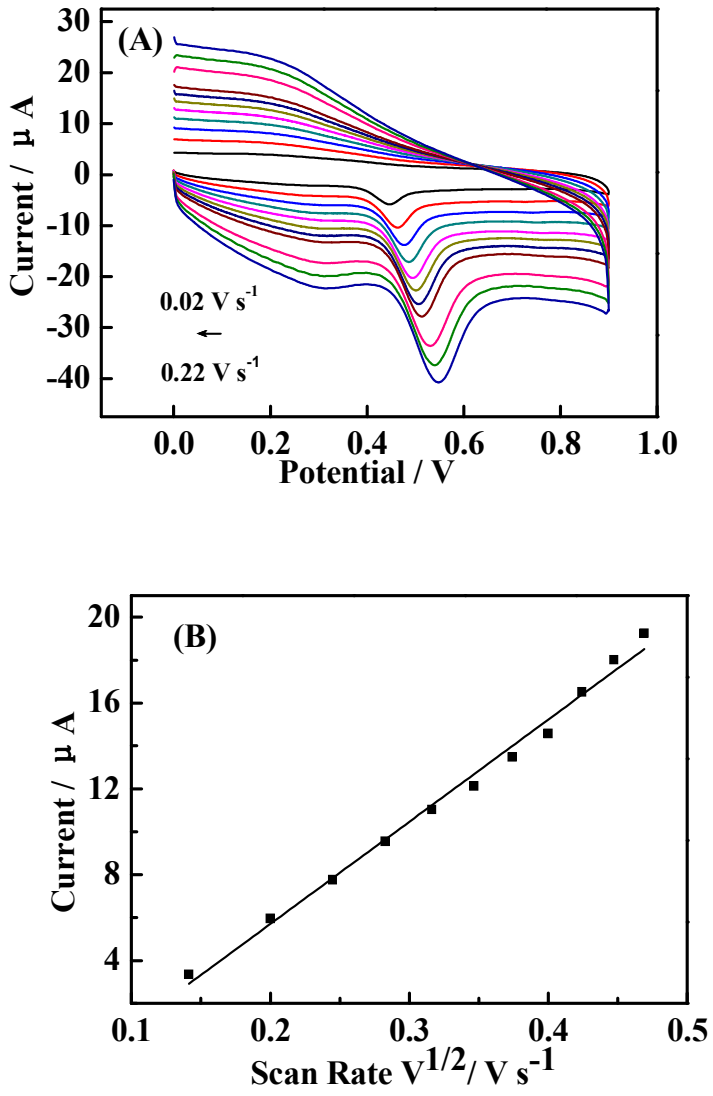

Fig.4 (A) Cyclic voltammograms of the GR/CA/GCE in 0.1 M PBS (pH 3.5) including 20 μM ISONIAZID at different scan rates (0.020-0.220 V s−1); (B) The linear dependence of peak current with the square root of scan rate.

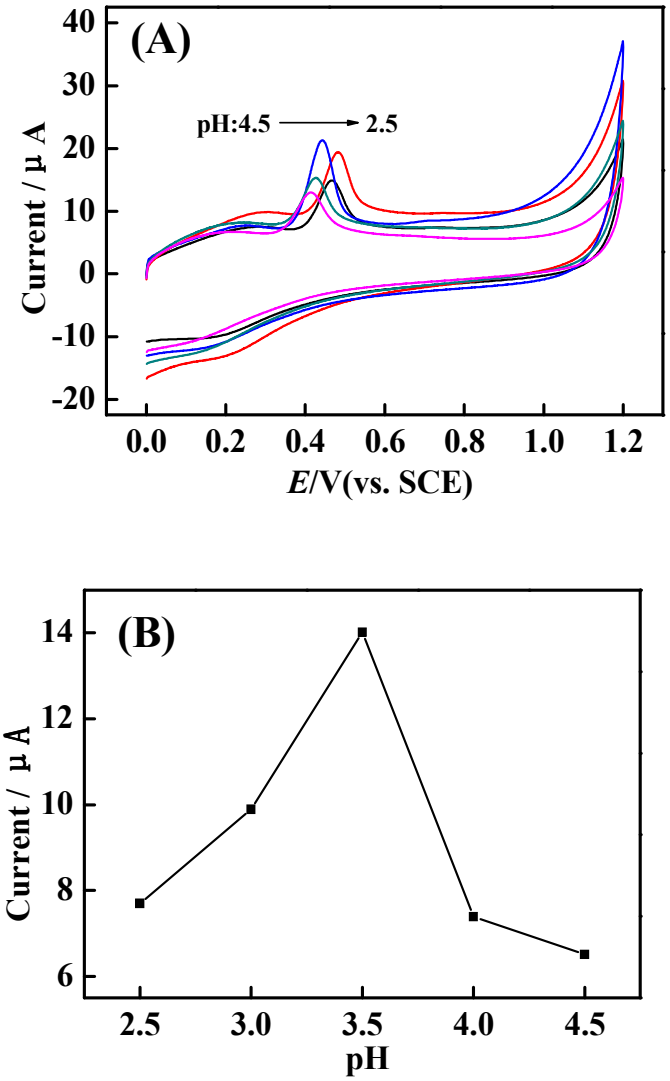

Fig. 5 (A) Cyclic voltammograms of 20 μM isoniazid in 0.1M PBS with various pH (from 4.5 to 2.5) at CA/ GR/GCE. (B) The effect of pH value on the oxidation current response of 20 μM isoniazid at CA/ GR/GCE.

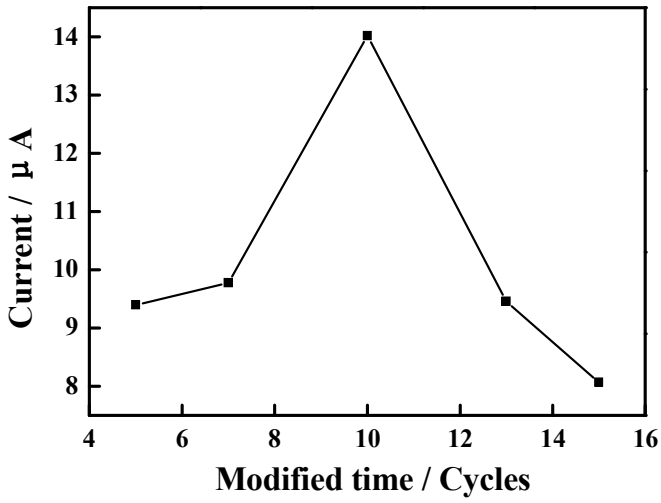

Fig. 6 Effect of electro-polymerization cycles of L-cysteine on the oxidation current response of 20 μM isoniazid.

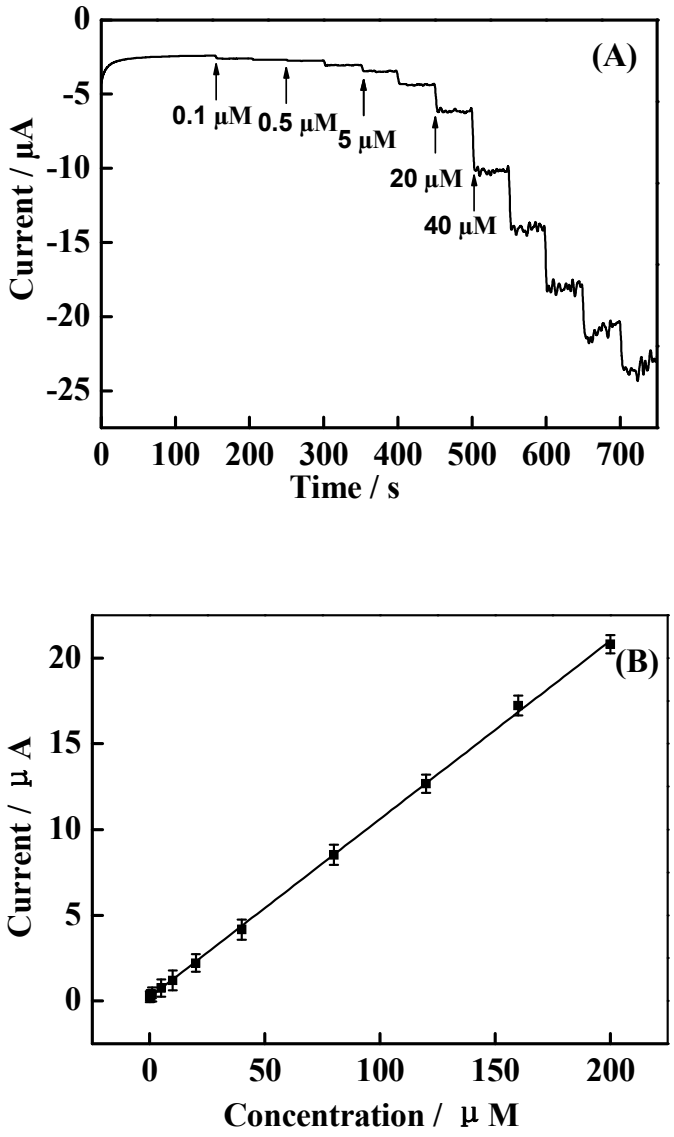

Fig. 7 (A) Current-time curve of GR/CA/GCE at different concentrations of isoniazid (0.1→200 μM); (B) The calibration curve for the determination of isoniazid.